

## IMAGE RESTORATION AND PHOTOMETRIC MONITORING OF THE GRAVITATIONAL LENS Q2237+0305

MARTIN HOUDE<sup>1</sup>

Canadian Marconi Company, Montréal H3P 1Y9, Canada

RENÉ RACINE

Département de Physique, Université de Montréal, Montréal H3C 3J7, Canada<sup>2</sup>

Electronic mail: racine@astro.umontreal.ca

Received 1993 June 9; revised 1993 September 24

### ABSTRACT

An image processing technique based on Lucy's algorithm [AJ, 79, 745 (1974)] was developed and tested on CCD frames of Q2237+0305 obtained at Observatoire du mont Mégantic on 1990 July 27 in FWHM  $\sim 1.5''$  seeing and on 1990 October 16 (FWHM  $\sim 1.7''$ ). Magnitudes were successfully obtained for the four components of this image which all lie within 1 arcsec of the lensing galaxy nucleus. Historical light curves (1986–1991) are constructed for the four images with the implementation of a "bootstrap" method. This also allows refinements to the estimates of differential extinction between the components and can detect microlensing events at the  $<0.1$  mag level. The results of our photometry agree well with the trends defined by other observations taken in superior seeing at the same epoch.

### 1. INTRODUCTION

The crowded appearance of the well-known gravitational lens Q2237+0305, four images of a  $z=1.695$  quasar around the core of the lensing galaxy, all within a radius of  $1''$  (Huchra *et al.* 1985; Yee 1988; DeRobertis & Yee 1988), would seem to permit accurate photometry of the components only when the seeing is significantly better than  $1''$  FWHM. We will show that by using the accurately known morphology of this object with the Lucy (1974) image restoration algorithm it is possible to extract photometrically correct images of the four components of the mirage from an originally blurred image. The technique is important here because it does allow reliable photometric monitoring of such objects under less than excellent seeing conditions. This is required if sufficient photometric coverage is to be obtained to unravel the physical properties of the source and lens on the basis of microlensing activity.

### 2. OBSERVATIONS AND IMAGE PROCESSING

Figures 1(a) and 1(b) show  $R$  images of Q2237+0305 obtained at the 1.6 m telescope of the Observatoire du mont Mégantic. The  $f/15$  configuration produced a sampling of  $0.26''/30 \mu\text{m}$  pixel on the RCA  $512 \times 320$  CCD. Figure 1(a) is the sum of four 200 s exposures and the PSF's FWHM is  $1.5''$ ; Fig. 1(b) sums seven 200 s frames with FWHM =  $1.7''$ . An inspection of these images shows that the structure of the central source is marginally non-stellar and that image processing could possibly be used to resolve and measure the magnitudes of the individual components of the quasar image. We will describe how Lucy's

algorithm (Lucy 1974) was used to produce restored images and illustrate the results obtained on the 1990 October 16 frames. Those from the 1990 July 27 observations are very similar.

We must first model the frame's PSF. To do so, we use star 2 (see Fig. 1). Its profile was found to be well represented by a Moffat (1969) function with a FWHM of  $1.7''$ . Once normalized, this is used as the PSF.

Lucy's method requires a first estimate of the solution as an input. Generally, when processing an image, the appropriate solution is not known and the amount of information that can be entered in the starting image is minimal. Fortunately, the case of Q2237+0305 is significantly different since its geometry is precisely known (Yee 1988, Racine 1991). We can take advantage of this in order to facilitate convergence toward the desired solution. The starting image can be generated using the known positions and some arbitrary magnitudes for the four components of the quasar image and the galaxy nucleus. These data and the relative positions of stars 1 and 2 are given in Table 1. The Gunn  $r$  magnitude of star 2 (Yee 1988) serves as a zero point for the determination of the components' magnitudes. It was found that the details of the intrinsic profile assumed for the components on the starting image had no influence on the resulting magnitudes; a Gaussian of FWHM  $0.45''$  was arbitrarily used.

Since we intend to measure the magnitudes of the components, it is preferable to subtract the lensing galaxy from the frame before processing. The latter was modeled using a de Vaucouleurs profile of ellipticity  $e=1-b/a=0.31$  with the major axis in P.A. of  $83^\circ$ . Its magnitude was adjusted to be  $r=16.75$  within a radius of  $2''$  (Racine 1991) before convolution with the PSF.

Once the starting image was completed, Lucy's method was applied to it. In order to reduce the computing time,

<sup>1</sup>Currently at Caltech Submillimeter Observatory, Hilo, HI.

<sup>2</sup>Also at Observatoire du mont Mégantic.

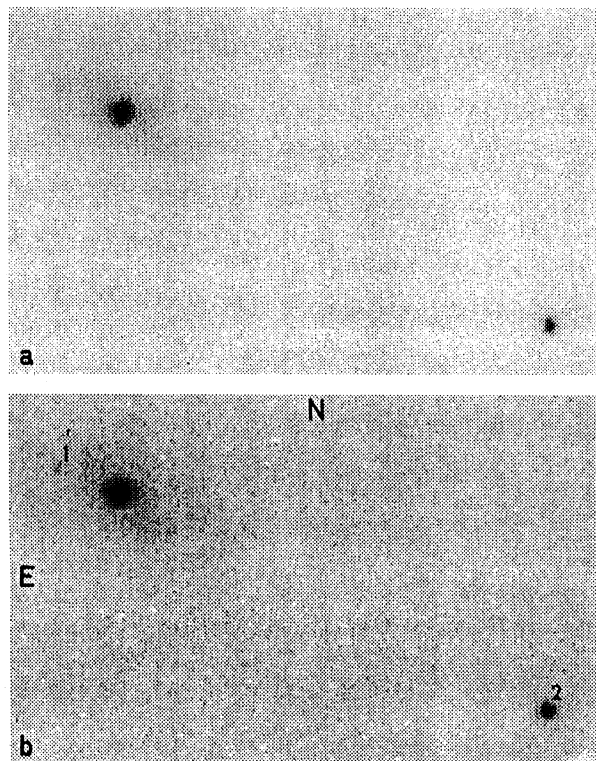


FIG. 1. Original images of Q2237+0305 obtained at mont Mégantic: (a) 1990 July 27, 1.5'' FWHM and (b) 1990 October 16, 1.7'' FWHM. The nonstellar morphology of the gravitational mirage is barely perceptible.

the processing was limited to a  $32 \times 32$  pixel subraster ( $\sim 8'' \times 8''$ ) of the original frames roughly centered on the galaxy nucleus. A correlation factor was calculated between two iterations far enough apart ( $\sim 200$  iterations) to estimate convergence. Solutions are shown in Fig. 2. The IRAF function `noao.artdata.magnify` is used here for display purposes, each pixel being replaced by  $4 \times 4$  others using a fifth-order polynomial for interpolation.

Figure 2(a) shows that the four components are completely resolved and that it is possible to measure their magnitudes with precision by simple aperture photometry. This was done with the IRAF task `testphot.apphot.qphot`. The sky level was taken to be the modal sky value in an annular region which excludes visible traces of the component images, and the aperture correction was determined from the known Gaussian profile of the image PSF. The

TABLE 1. Starting positions and magnitudes used for processing.

| Id.     | Positions                |                          | mag ( $r$ )        |
|---------|--------------------------|--------------------------|--------------------|
|         | $\Delta\alpha(^{\circ})$ | $\Delta\delta(^{\circ})$ |                    |
| A       | 0.00                     | 0.00                     | 17.62              |
| B       | -0.67                    | +1.68                    | 17.52              |
| C       | +0.62                    | +1.20                    | 18.21              |
| D       | -0.86                    | +0.53                    | 18.41              |
| nucleus | -0.08                    | 0.94                     | 16.75 <sup>a</sup> |
| 1       | +7.90                    | +4.30                    | 19.38              |
| 2       | -57.10                   | -27.90                   | 17.44              |

<sup>a</sup> in a  $2''$  radius before convolution

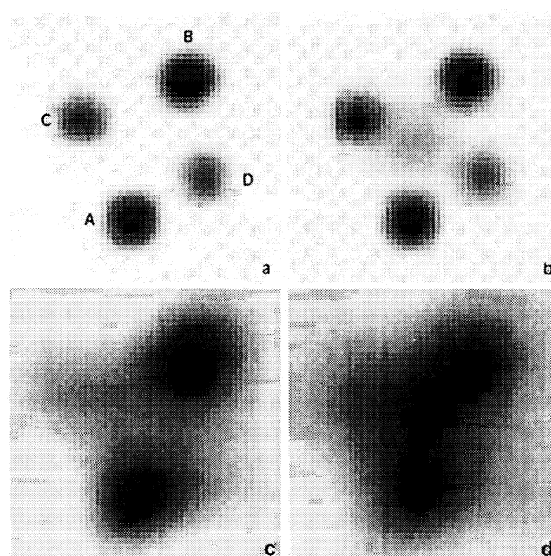


FIG. 2. (Top) Images of Q2237+0305 after processing with galaxy subtracted (left) and present (right) in the original frame. In both cases the starting image contained a maximum of morphological information. (Bottom) Same as above but with a starting image containing no information. These frames are 3 arcsec on a side.

results are given in the third column of Table 2(b). Figure 2(b) was obtained without first subtracting the galaxy nucleus. Rather its model, described earlier, was included in the starting image.

It is interesting to see what happens when no information is entered in the starting image. The results thus obtained are shown in Figs. 2(c) and 2(d). Note that even if the components are not fully restored we can still recognize the general morphology of the mirage.

### 3. ROBUSTNESS OF THE METHOD AND UNCERTAINTIES

Even though the pictorial results shown in Fig. 2 appear conclusive, we must make sure that the photometric solution does not depend critically on the information contained in the starting image. To test this we have tried

TABLE 2. Tests of robustness.  
a) adopted magnitudes for the starting image

| Id. | 1     | 2     | 3     | 4     | 5     |
|-----|-------|-------|-------|-------|-------|
| A   | 19.02 | 18.27 | 17.62 | 16.77 | 16.02 |
| B   | 19.02 | 18.27 | 17.52 | 16.77 | 16.02 |
| C   | 19.02 | 18.27 | 18.21 | 16.77 | 16.02 |
| D   | 19.02 | 18.27 | 18.41 | 16.77 | 16.02 |

b)  $r$  magnitudes after convergence (90.07.27)

| Id. | 1     | 2     | 3     | 4     | 5     | $r_f$ | $\sigma$ |
|-----|-------|-------|-------|-------|-------|-------|----------|
| A   | 17.72 | 17.70 | 17.68 | 17.68 | 17.67 | 17.69 | 0.02     |
| B   | 17.65 | 17.63 | 17.61 | 17.61 | 17.61 | 17.62 | 0.02     |
| C   | 18.12 | 18.09 | 18.09 | 18.04 | 18.02 | 18.09 | 0.03     |
| D   | 18.63 | 18.58 | 18.60 | 18.57 | 18.50 | 18.61 | 0.04     |

c)  $r$  magnitudes after convergence (90.10.16)

| Id. | 1     | 2     | 3     | 4     | 5     | $r_f$ | $\sigma$ |
|-----|-------|-------|-------|-------|-------|-------|----------|
| A   | 17.77 | 17.81 | 17.73 | 17.77 | 17.72 | 17.76 | 0.03     |
| B   | 17.57 | 17.56 | 17.49 | 17.50 | 17.45 | 17.51 | 0.02     |
| C   | 18.19 | 18.18 | 18.16 | 18.13 | 18.07 | 18.17 | 0.02     |
| D   | 18.44 | 18.42 | 18.45 | 18.27 | 18.20 | 18.42 | 0.04     |

widely different starting magnitudes for the components. First we assigned to each component the magnitudes measured by Racine (1991) [Table 2(a), starting model 3]. We then assigned to each component the magnitude of image  $B$  divided and multiplied by factors of 2 and 4 [Table 2(a)]. Lucy's method was applied to each of these cases. The following criteria had to be met for the solution to be acceptable: (1) there must be convergence; (2) each component must not have been displaced by more than 0.25 pixel (0.06"); (3) the final image must be morphologically consistent with the numerous observations of Q2237+0305: the quasar's components (and noise) must be the only features present in the image.

Each of these requirements was satisfied in every case, therefore demonstrating the robustness of the technique. These tests also provide estimates of the systematic biases and random errors in the magnitudes that may be introduced by the image processing itself. It will be noted that the output magnitudes in Tables 2(b) and 2(c) show shallow linear dependence on the input magnitudes, with slopes ranging from 0.02 mag/mag for the brighter components  $A$  and  $B$  to 0.09 mag/mag for the faintest component  $D$  on the July frame and with dispersions  $\sigma_1$  averaging 0.012 mag. To eliminate the biases, it is sufficient to read the interpolated value of the final magnitude corresponding to the same input magnitude to obtain a final value  $r_f$  given in the Table. The dispersion  $\sigma$  is an indication of the random errors of the image restoration process. The statistical uncertainties ( $\sigma_2$ ) due to photon noise in the images were evaluated for each component from the signal-to-noise ratio obtained by dividing the net component flux after processing by the photon noise of the flux contained within the *original* FWHM centered on the component (including background and galaxy light). Combining  $\sigma_1$  and  $\sigma_2$  quadratically gives the total uncertainty  $\sigma$ . Tables 2(b) and 2(c) give the results obtained from the two sets of Méganitic observations along with the uncertainties in the last column. The results for components  $C$  and  $D$  are less secure, being fainter and more deeply embedded in the galaxy bar than  $A$  and  $B$ . That the two independent sets of results agree reasonably well with one another when their uncertainties are taken into account is a further indication of their validity.

Of course, from the very nature of the phenomenon, luminosity changes between epochs are expected, either through changes in the source or by microlensing, and a more telling comparison should be based on the otherwise known brightness trends observed in the fall of 1990. We now turn to the question of defining microlensing light curves for the components of this gravitational mirage.

#### 4. CONSTRUCTION OF HISTORICAL LIGHT CURVES

A number of photometric observations of Q2237+0305 have been published [see Corrigan *et al.* (1991), for a partial compilation]. The data are often obtained during the course of other programs and are quite inhomogeneous as to bandpasses, reduction, and calibration procedures. The interpretation of microlensing events require well-sampled

and photometrically consistent light curves over intervals of many years (Wambsganns *et al.* 1990). A "bootstrap" method will now be outlined whereby data taken in different bandpasses can be freed from zero-point differences and combined into a single light curve for each component.

Two assumptions are made about the properties of the images: (1) All four have identical intrinsic color indices; their observed color differences are due to different degrees of interstellar extinction and reddening by the same extinction law. (2) At a given epoch, the magnitude difference between one of the images and the mean of all four is a constant, which can be estimated from its average over time, to which is superimposed a variable micro(de)amplification  $\Delta m_p$ . The first assumption must be valid in the absence of microlensing. It would fail during an event if the source size is wavelength dependent and resolved by the microcaustic. Thus, wavelength dependent deviations from the mean light curve of an event could reveal colored structures in the source. This would be particularly noticeable if there were an emission line, due to the quasar envelope or broadline region, in the band (Racine 1992). The second assumption would fail if the source brightness varied significantly during the time delay between images. For Q2237+0305 these delays are <0.5 day (Kent & Falco 1988; Rix *et al.* 1992) and QSO variations in excess of a few percent during such short intervals are unlikely. Since this second assumption is also used to reconcile the zero points of the various photometric series, global source variability is erased.

The procedure is as follows.

(1) An extinction law  $A(\lambda)$  (Nadeau *et al.* 1991, Fig. 7), presumably due to the lensing galaxy, is adopted. It is given by the ratio of total to selective extinction

$$R(\lambda) = A(\lambda)/E(g-i) \\ = 1.33 (\lambda_{\mu\text{m}}^{-1} - 1.5) - 0.22 (\lambda_{\mu\text{m}}^{-1} - 1.5)^3 + 1.25$$

and yields  $A_V/E(B-V) = 3.2$  Yee's (1988)  $(g-i)$  colors of the component indicate differential reddenings  $\Delta E(g-i)$  with respect to image  $A$  of +0.08 for  $B$ , +0.33 for  $C$ , and +0.19 for  $D$ . The published magnitudes  $m_i(\lambda)$  are all reduced to the extinction of  $A$  by  $m_{c,i}(\lambda) = m_i(\lambda) - R(\lambda)\Delta E(g-i)$ . These corrections for differential extinction should make the magnitude differences between components independent of wavelength.

(2) The mean of the extinction-corrected magnitudes of the four components is computed at each epoch and, for each bandpass, a light curve is plotted. These curves are superimposed to better define trends in the mean magnitude which are due to QSO variability or microlensing activity. The effect of the latter is, of course, reduced by averaging at each epoch. A smooth light curve drawn through these mean magnitudes reduces the "noise" due to differences in photometric calibration and reduction and provides, for each epoch, a quantity  $\Delta\langle m_0 \rangle$  which describes how the mean magnitude  $\langle m_0 \rangle$  differs from its long-term value. These  $\Delta\langle m_0 \rangle$  values are found in Table 3, column 8.

TABLE 3. Photometry and variability in Q2237+0305.

| Epoch    | $\lambda(\mu\text{m})^1$ | Magnitudes |       |       |       | Ref. | $\Delta\langle m_0 \rangle$ | Relative Magnitudes |            |            |            |
|----------|--------------------------|------------|-------|-------|-------|------|-----------------------------|---------------------|------------|------------|------------|
|          |                          | A          | B     | C     | D     |      |                             | $\Delta A$          | $\Delta B$ | $\Delta C$ | $\Delta D$ |
| 1986.743 | 1.44                     | 17.48      | 17.42 | 17.81 | 18.27 | 1    | -0.04                       | -0.11               | -0.28      | -0.14      | 0.37       |
| 1986.743 | 1.81                     | 17.43      | 17.32 | 17.81 | 18.36 | 1    | -0.04                       | -0.07               | -0.33      | -0.19      | 0.43       |
| 1987.735 | 1.55                     | 17.45      | 17.65 | 17.90 | 18.24 | 2    | 0.02                        | -0.13               | -0.04      | -0.07      | 0.32       |
| 1987.735 | 1.22                     | 17.25      | 17.40 | 17.55 | 17.95 | 2    | 0.02                        | -0.12               | -0.05      | -0.09      | 0.35       |
| 1987.735 | 2.00                     | 17.90      | 18.09 | 18.41 | 18.57 | 2    | 0.02                        | -0.02               | 0.00       | -0.07      | 0.26       |
| 1987.743 | 1.81                     | 17.62      | 17.83 | 18.08 | 18.53 | 1    | 0.02                        | -0.11               | -0.04      | -0.14      | 0.37       |
| 1988.533 | 1.55                     | 17.31      | 17.64 | 17.95 | 18.16 | 1    | 0.00                        | -0.24               | -0.03      | 0.00       | 0.27       |
| 1988.563 | 0.80                     | 15.89      | 16.01 | 16.18 | 16.53 | 3    | 0.00                        | -0.20               | -0.11      | -0.03      | 0.34       |
| 1988.563 | 0.61                     | 15.26      | 15.42 | 15.53 | 15.79 | 3    | 0.00                        | -0.20               | -0.06      | 0.00       | 0.27       |
| 1988.563 | 0.45                     | 14.91      | 15.02 | 15.09 | 15.47 | 3    | 0.00                        | -0.19               | -0.09      | -0.05      | 0.34       |
| 1988.600 | 1.55                     | 17.32      | 17.63 | 17.89 | 18.23 | 1    | -0.03                       | -0.26               | -0.07      | -0.09      | 0.30       |
| 1988.633 | 1.44                     | 17.16      | 17.63 | 17.97 | 18.16 | 1    | -0.03                       | -0.41               | -0.05      | 0.05       | 0.29       |
| 1988.633 | 2.27                     | 17.85      | 18.35 | 18.92 | 19.11 | 1    | -0.03                       | -0.38               | -0.08      | 0.03       | 0.31       |
| 1988.691 | 2.27                     | 17.88      | 18.35 | 18.92 | 19.24 | 1    | -0.03                       | -0.39               | -0.12      | -0.01      | 0.40       |
| 1988.694 | 2.27                     | 17.89      | 18.45 | 18.84 | 19.33 | 1    | -0.03                       | -0.41               | -0.05      | -0.12      | 0.46       |
| 1988.711 | 1.44                     | 17.17      | 17.63 | 17.99 | 18.16 | 1    | -0.03                       | -0.41               | -0.05      | 0.06       | 0.28       |
| 1988.711 | 2.27                     | 17.88      | 18.38 | 18.92 | 19.25 | 1    | -0.03                       | -0.40               | -0.10      | -0.02      | 0.40       |
| 1988.711 | 1.81                     | 17.23      | 17.81 | 18.14 | 18.34 | 1    | -0.03                       | -0.41               | 0.02       | 0.00       | 0.27       |
| 1988.866 | 1.55                     | 17.32      | 17.67 | 17.97 | 18.23 | 1    | -0.03                       | -0.27               | -0.04      | -0.02      | 0.29       |
| 1988.866 | 1.22                     | 17.19      | 17.56 | 17.79 | 18.15 | 1    | -0.03                       | -0.35               | -0.06      | -0.01      | 0.38       |
| 1988.866 | 2.27                     | 17.99      | 18.44 | 18.85 | 19.29 | 1    | -0.01                       | -0.31               | -0.05      | -0.10      | 0.43       |
| 1988.866 | 2.00                     | 17.67      | 18.06 | 18.39 | 18.71 | 1    | -0.01                       | -0.24               | -0.02      | -0.09      | 0.31       |
| 1989.508 | 2.27                     | 17.85      | 18.39 | 19.01 | 19.13 | 1    | -0.02                       | -0.41               | -0.07      | 0.10       | 0.30       |
| 1989.597 | 1.44                     | 17.30      | 17.62 | 18.07 | 18.20 | 1    | 0.03                        | -0.28               | -0.06      | 0.14       | 0.32       |
| 1989.597 | 2.27                     | 18.00      | 18.40 | 19.11 | 19.18 | 1    | 0.03                        | -0.29               | -0.08      | 0.17       | 0.33       |
| 1989.600 | 1.44                     | 17.32      | 17.63 | 18.07 | 18.20 | 1    | 0.03                        | -0.26               | -0.06      | 0.13       | 0.31       |
| 1989.600 | 2.27                     | 18.00      | 18.12 | 18.75 | 18.87 | 1    | 0.03                        | -0.05               | -0.13      | 0.05       | 0.25       |
| 1989.680 | 1.44                     | 17.30      | 17.66 | 18.14 | 18.21 | 1    | 0.03                        | -0.31               | -0.05      | 0.18       | 0.30       |
| 1989.680 | 2.27                     | 17.97      | 18.38 | 19.02 | 19.03 | 1    | 0.03                        | -0.25               | -0.03      | 0.15       | 0.25       |
| 1989.680 | 1.44                     | 17.31      | 17.64 | 18.14 | 18.18 | 1    | 0.03                        | -0.29               | -0.06      | 0.19       | 0.28       |
| 1989.683 | 2.27                     | 17.99      | 18.38 | 18.97 | 19.00 | 1    | 0.03                        | -0.21               | -0.02      | 0.12       | 0.23       |
| 1989.683 | 1.44                     | 17.50      | 17.68 | 18.10 | 18.16 | 1    | 0.03                        | -0.14               | -0.07      | 0.11       | 0.22       |
| 1989.802 | 2.27                     | 18.28      | 18.48 | 19.11 | 19.06 | 1    | 0.07                        | -0.03               | -0.02      | 0.15       | 0.19       |
| 1989.805 | 1.55                     | 17.51      | 17.62 | 18.07 | 18.13 | 1    | 0.07                        | -0.04               | -0.05      | 0.13       | 0.24       |
| 1989.805 | 2.27                     | 18.29      | 18.43 | 19.13 | 19.04 | 1    | 0.07                        | -0.01               | -0.06      | 0.18       | 0.18       |
| 1989.808 | 1.55                     | 17.51      | 17.65 | 18.09 | 18.13 | 1    | 0.07                        | -0.05               | -0.03      | 0.13       | 0.23       |
| 1989.808 | 2.27                     | 18.25      | 18.38 | 19.06 | 19.03 | 1    | 0.07                        | -0.01               | -0.07      | 0.15       | 0.21       |
| 1989.810 | 1.55                     | 17.51      | 17.67 | 18.11 | 18.18 | 1    | 0.07                        | -0.07               | -0.03      | 0.13       | 0.25       |
| 1989.824 | 1.81                     | 17.74      | 17.90 | 18.38 | 18.62 | 1    | 0.07                        | -0.08               | -0.07      | 0.06       | 0.37       |
| 1989.985 | 2.27                     | 18.35      | 18.43 | 18.98 | 19.09 | 1    | 0.05                        | 0.04                | -0.07      | 0.02       | 0.22       |
| 1990.571 | 1.44                     | 17.69      | 17.62 | 18.09 | 18.56 | 4    | 0.08                        | -0.03               | -0.21      | 0.02       | 0.54       |
| 1990.646 | 1.06                     | 16.80      | 16.68 | 17.32 | 17.53 | 5    | 0.08                        | -0.09               | -0.27      | 0.22       | 0.46       |
| 1990.646 | 1.55                     | 17.62      | 17.52 | 18.21 | 18.41 | 5    | 0.08                        | -0.03               | -0.24      | 0.17       | 0.42       |
| 1990.660 | 2.00                     | 17.74      | 17.60 | 18.41 | 18.62 | 6    | 0.08                        | 0.03                | -0.28      | 0.14       | 0.42       |
| 1990.660 | 2.27                     | 17.96      | 17.82 | 18.66 | 18.98 | 6    | 0.08                        | 0.04                | -0.30      | 0.09       | 0.49       |
| 1990.794 | 1.44                     | 17.76      | 17.51 | 18.17 | 18.36 | 4    | 0.05                        | 0.05                | -0.31      | 0.11       | 0.35       |
| 1990.966 | 1.44                     | 17.42      | 17.29 | 18.11 | 18.34 | 7    | 0.03                        | -0.15               | -0.39      | 0.19       | 0.47       |
| 1990.966 | 2.78 <sup>a</sup>        | 16.63      | 16.53 | 17.56 | 17.97 | 7    | 0.03                        | -0.11               | -0.43      | 0.07       | 0.58       |
| 1991.771 | 1.81                     | 17.36      | 17.01 | 18.10 | 18.16 | 8    | -0.03                       | -0.06               | -0.56      | 0.18       | 0.31       |

<sup>a</sup> instrumental magnitudes

## Notes to TABLE 3

<sup>1</sup>Corrigan *et al.* (1991).<sup>2</sup>Racine (1991).<sup>3</sup>Yee (1988).<sup>6</sup>Crane *et al.* (1991).<sup>4</sup>Nadeau *et al.* (1991).<sup>7</sup>Rix *et al.* (1992).<sup>5</sup>This paper.<sup>8</sup>Racine (1992).

(3) Finally, for each epoch, we compute the differences  $\Delta m_i$  between the magnitudes of each image and the mean magnitude of the four images from which  $\Delta\langle m_0 \rangle$  had been subtracted. Variations in these differences, which are due to microlensing, are unaffected by the zero-point variations between datasets, which produce considerable scatter in the mean light curves obtained at step (2).

If the adopted  $\Delta E(g-i)$ 's or the extinction law were incorrect, the  $\Delta m_i$ 's would show trends with wavelength even without coloration due to microlensing. The many data points for *B*, *C*, and *D* in 1988 and 1989 (no strong photometric activity indicated) were used for testing and did reveal small but significant slopes  $\partial\Delta m_i/\partial(1/\lambda_{\mu\text{m}})$  ( $\pm 0.007$ ) of  $-0.015$  for *B*,  $+0.040$  for *C*, and  $-0.095$  for *D*. Since these values are not proportional to the color excesses—which they would be if the extinction law was incorrect—the  $\Delta E(g-i)$ 's themselves must require (small) adjustments: from 0.08 to 0.09 for *B*, from 0.33 to 0.30 for *C*, and from 0.19 to 0.26 for *D*. These are within the uncertainties of Yee's photometry.

Table 3 gives the photometry log and the resulting  $\Delta m_i$  values. Figure 3 shows the light curves. The photometric accuracy appears to be typically  $\pm 0.03$  mag for *A* and *B* and  $\pm 0.05$  mag for *C* and *D*, with a few stray data points. Strong amplification events are seen for *A* between 1988.5

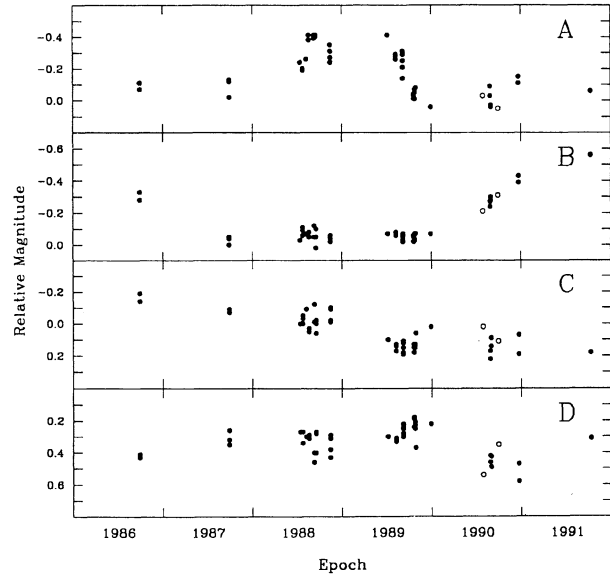


FIG. 3. Historical light curves for the four components of Q2237+0305 obtained by the method described in Sec. 4. Microlensing effects are apparent. The open symbols result from the present photometry of Lucy-deconvolved images.

and 1989.7 ( $\Delta m_{\text{max}} \sim 0.35$  mag; Irwin *et al.* 1989, Nadeau *et al.* 1991, Corrigan *et al.* 1991) and in *B* starting at  $\sim 1990.0$  ( $\Delta m_{\text{max}} = 0.50$ ; Petersen 1990, Racine 1991). Image *C* has become gradually fainter by  $\sim 0.35$  mag between 1986 and 1990 while *D* appears stable to within 0.1 mag except for a  $\sim 0.15$  mag drop in 1990. Microlensing is seen to be ubiquitous in Q2237+0305 and characterized by variations of  $< 0.6$  mag. Rapid (1–2 month, e.g., *A* in  $\sim 1989.7$ ) and slow (a few years, e.g., *B* and *C*) light modulations are observed. The data show no systematic coloration during amplification [ $\partial\Delta m_i/\partial(1/\lambda_{\mu\text{m}}) < 0.03$ ]. This suggests that the continuum source seen in these broadband observations has uniform color over the scale of the microcaustic structures. On the other hand, the line-emitting region is known to be much less sensitive to microlensing and must be larger than the microcaustics (Racine 1992). The results from our photometry of the Lucy-restored M3 images are shown as open symbols in Fig. 3 and are seen to conform well to the historical light curves. This confirms the reliability and usefulness of this type of photometry.

## 5. CONCLUSIONS

An image processing technique was developed to extract photometric information from frames of Q2237+0305 taken under quite average seeing conditions (FWHM =  $1.5''$ – $1.7''$ ). It was demonstrated that using the available knowledge of the morphology of this object facilitates the convergence of a solution which is photometri-

cally reliable. The technique is robust with respect to quite large variations of the starting parameters and the results are consistent with independent photometry of the source components. It is therefore possible to carry out useful photometric monitoring of challenging complex sources such as Q2237+0305 in a routine manner under quite average seeing conditions.

M.H. acknowledges support from a NSERC scholarship and from Canadian Marconi Company, which allowed him to take a leave of absence during which most of this research was done. We thank Michel Rivard who took the 1990 July 27 images. This work was supported in part through grants to R.R. from NSERC and from Fonds FCAR. Québec.

## REFERENCES

- Corrigan, R. T., *et al.* 1991, AJ, 102, 34  
Crane, P., *et al.* 1991, ApJ, 369, 59  
DeRobertis, M. M., & Yee, H. K. C. 1988, ApJ, 332, L49  
Huchra, J., Gorenstein, M., Kent, S., Shapiro, I., Smith, G., Horine, E., & Perley, R. 1985, AJ, 90, 691  
Irwin, M. J., Webster, R. L., Hewett, P. C., Corrigan, R. T., & Jedrzejewski, R. I. 1989, AJ, 98, 1989  
Kent, S. M., & Falco, E. E. 1988, AJ, 96, 1570  
Lucy, L. B. 1974, AJ, 79, 745  
Moffat, A. F. J. 1969, A&A, 3, 455  
Nadeau, D., Yee, H. K. C., Forrest, W., Garnett, J., Ninkov, Z., & Pipher, J. 1991, ApJ, 376, 430  
Petersen, B. R. 1990, IAU Circ. No. 5099  
Racine, R. 1991, AJ, 102, 454  
Racine, R. 1992, ApJ, 395, L65  
Rix, H.-W., Schneider, D. P., & Bahcall, J. N. 1992, AJ, 104, 959  
Wambsganns, J., Paczynski, B., & Schneider, D. P. 1991, ApJ, 358, L33  
Yee, H. K. C. 1988, AJ, 95, 1331